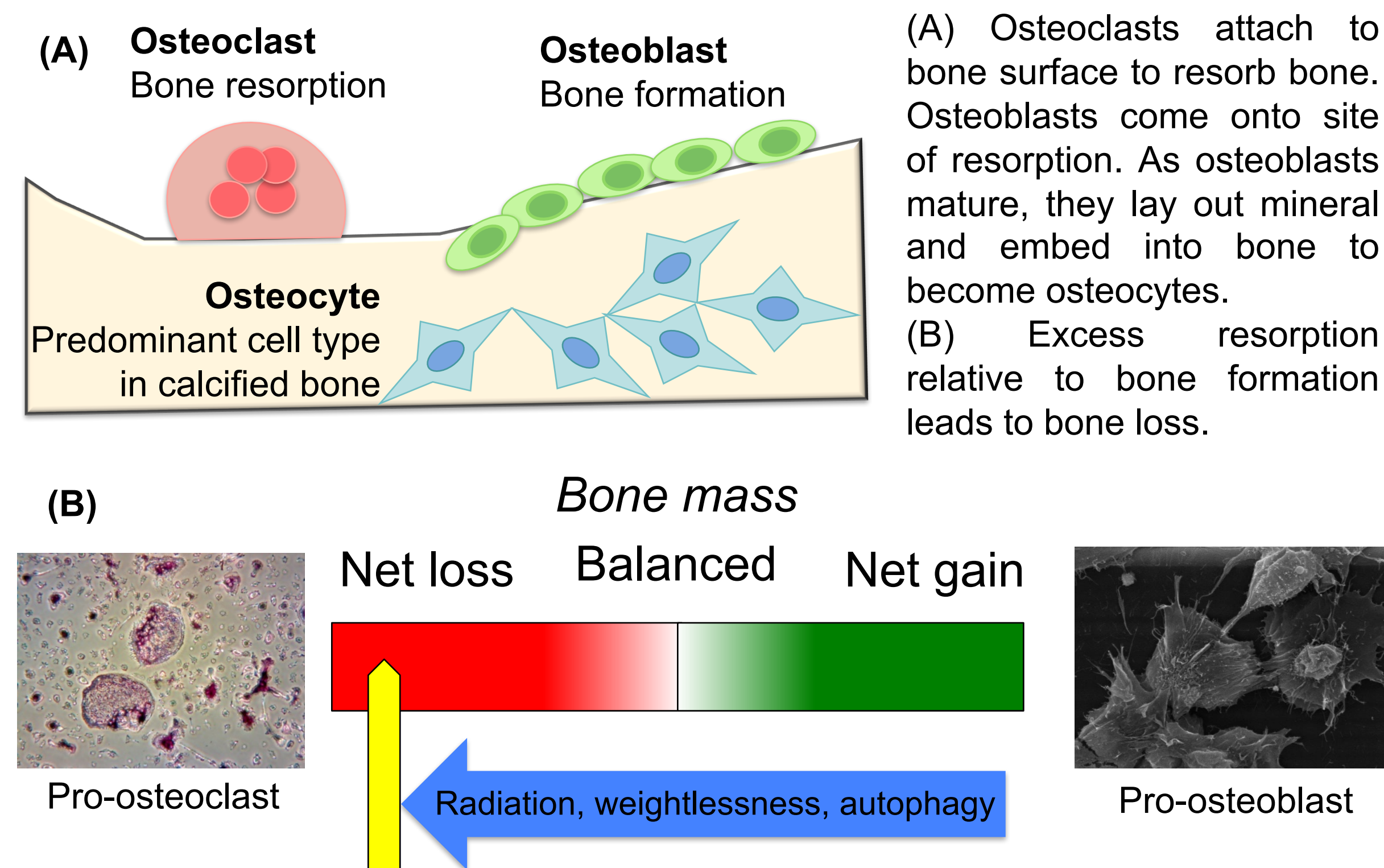


Abstract
Weightlessness and radiation, two unique elements of space, profoundly decreases bone mass. This bone loss is attributed to increased activity of bone-resorbing osteoclasts and functional changes in bone-forming osteoblasts, cells that give rise to mature osteocytes. Our long-term goal is to identify signaling pathways that may be targeted to mitigate bone loss in scenarios of space exploration, radiotherapy and accidental radiation exposure. We have previously shown that exposure of MLO-Y4 osteocyte-like cells to simulated space radiation (⁶⁰Fe) increased the expression of the pro-osteoclastogenic gene rankl and decreased protein levels of LC3B-II, a key player in autophagy. In this current study, we aimed to further elucidate the role of autophagy in maintaining structural integrity of the skeleton. We hypothesize that loss of autophagy in bone leads to an imbalance in pro-osteoclastogenic and pro-osteogenic signals, resulting in net bone loss. To test our hypothesis we performed global postnatal deletion of Atg12 using tamoxifen-inducible Cre recombinase under the control of the CAG promoter. Six-week-old CAG-CreERT2/FloxAtg12 animals were treated daily with Tamoxifen or Vehicle (Control, oil only) for five days and euthanasia performed two weeks after the onset of treatment. Percent change in body weights (prior to treatment and at euthanasia) was not significantly different between treatment groups within the same gender. Compared to Vehicle (Control) groups, Tamoxifen (Atg12 iKO) groups showed decreased LC3B-I to II conversion and increased p62 protein levels, consistent with loss of autophagy. Quantitative PCR revealed increased expression of pro-osteoclastogenic cytokines mcp1 and rankl in bone and marrow respectively in male iKOs compared to male controls. Expression levels of these genes were not significantly altered in the Atg12 iKO females compared to female controls. Microcomputed tomography of tibiae revealed decreased cortical bone volume, cortical thickness and periosteal perimeter consistent with bone loss; and a longer primary spongiosa in male Atg12 iKOs compared to male controls. These decrements were less pronounced in the female Atg12 iKOs. Cancellous bone structure was not significantly different between iKOs and controls in both genders. Histological analysis also revealed that compared to male controls, male iKOs showed a profound increase in chondrocyte column length of the growth plate with hyper-expansion of both proliferating and hypertrophic zones. Taken together, these findings indicate that autophagy plays an important role in the maintenance of bone structural integrity by mediating the production of pro-osteoclastogenic signals and regulating chondrocyte proliferation and differentiation.

INTRODUCTION

Major cell types involved in skeletal homeostasis



Molecular mechanisms of bone loss

Underlying mechanisms include increase in pro-osteoclastogenic (pro-resorption) signals and increased reactive oxygen species (ROS) with resulting oxidative stress in bone. Accumulation of oxidative damage in osteoblasts and osteocytes can lead to cell death, which in turn may also contribute to bone loss.

Role of autophagy in bone

Macroautophagy (referred to here as “autophagy”) is a process by which organelles are broken down and recycled for use in new cellular components and signaling events.

Deletion of Atg7 in osteocytes leads to osteopenia (Onal et al. 2013).

PURPOSE OF THE STUDY

Determine the consequences of global loss of Atg12 on skeletal integrity and bone homeostasis; elucidate underlying mechanisms.

P2324: Atg12 maintains skeletal integrity by modulating pro-osteoclastogenic signals and chondrocyte differentiation

Candice Tahimic^{1,2}, Disha Bahl¹, Yasaman Shirazi-Fard¹, Timothy Marsh³, Ann-Sofie Schreurs¹, Victoria E. Rael^{4,5}, Chloe Glikbarg¹, Jayantha Debnath³ and Ruth K. Globus¹

¹Space Biosciences Division, NASA Ames Research Center; ²Wyle Laboratories; ³School of Medicine, Department of Pathology, University of California at San Francisco; ⁴Space Life Sciences Training Program (SLSTP), NASA Ames Research Center, ⁵Biological Sciences Collegiate Division, University of Chicago, IL

MATERIALS AND METHODS

Atg 12 knockout studies:

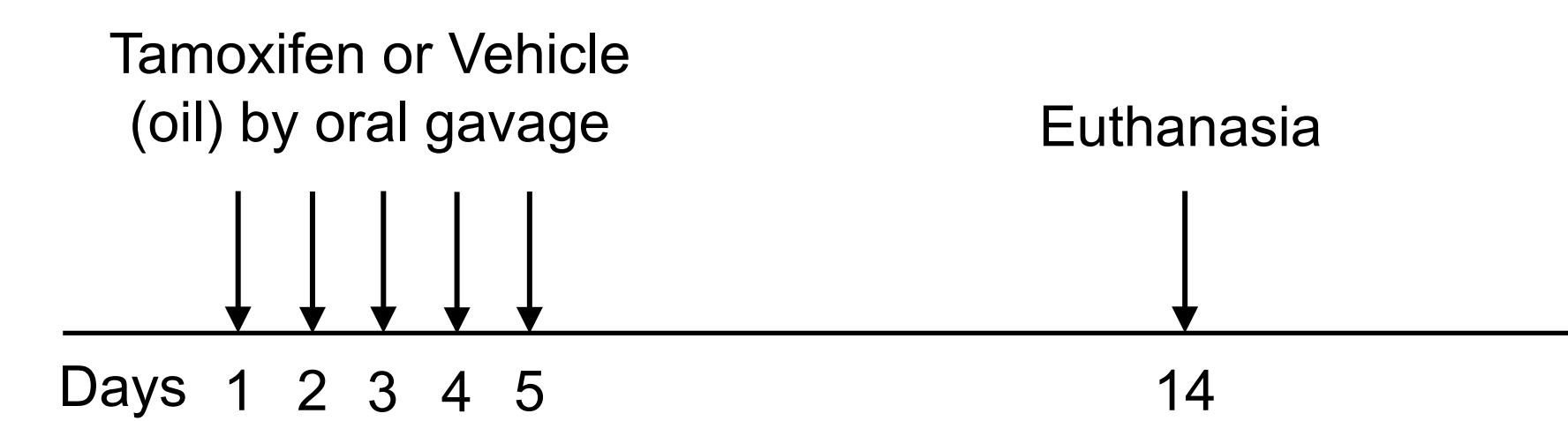
Strain: CAG-Cre^{ERT2} / Atg12^{flox/flox} in C57BL/6 background

Age at onset of Tamoxifen treatment: 6 weeks (1.5 months)

Age at euthanasia: 8 weeks

Samples collected: femora and tibiae

All animal procedures were performed with IACUC pre-approval.



Quantitative PCR (qPCR): RNA extraction of femur was performed using Trizol method and cDNA generated. Relative gene expression levels were calculated using the $\Delta\Delta Ct$ method with *Rpl19* as internal control.

Analysis of skeletal microarchitecture: Microcomputed tomography of tibia was performed using Skyscan platform (Bruker) at resolutions of 6.7 and 15 μm for cancellous and cortical bone respectively.

Histology: Tissues were fixed in 4% paraformaldehyde and processed for paraffin sectioning. Safranin O stain was performed to visualize chondrocytes.

RESULTS

Body mass and treatment effects

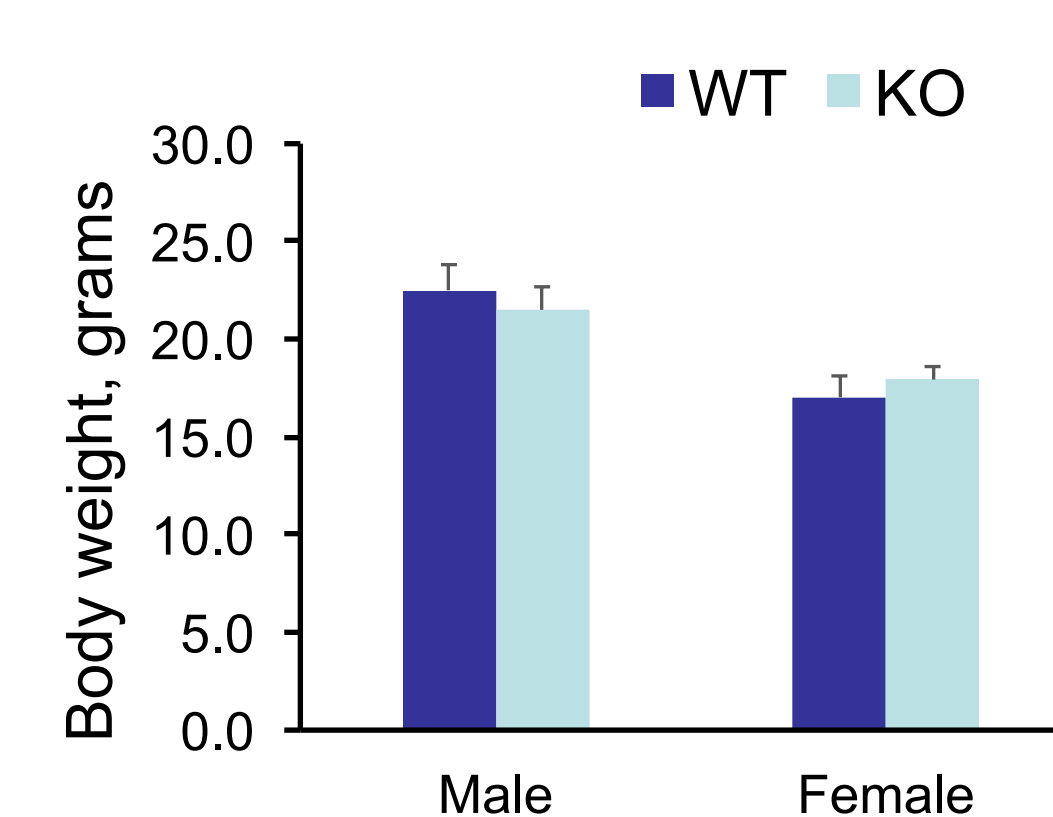


Figure 1. Body mass of groups prior to treatment. Male and females CAG-Cre^{ERT2}/Atg12^{flox/flox} mice were divided into groups that were to receive vehicle (WT) or tamoxifen treatment (KO). Values depicted are means; N=3-4/group. Error bars indicate SD; Wild type and KO groups within a gender had similar body weights at onset of treatment. One-way ANOVA showed gender effects in pre-treatment body weights.

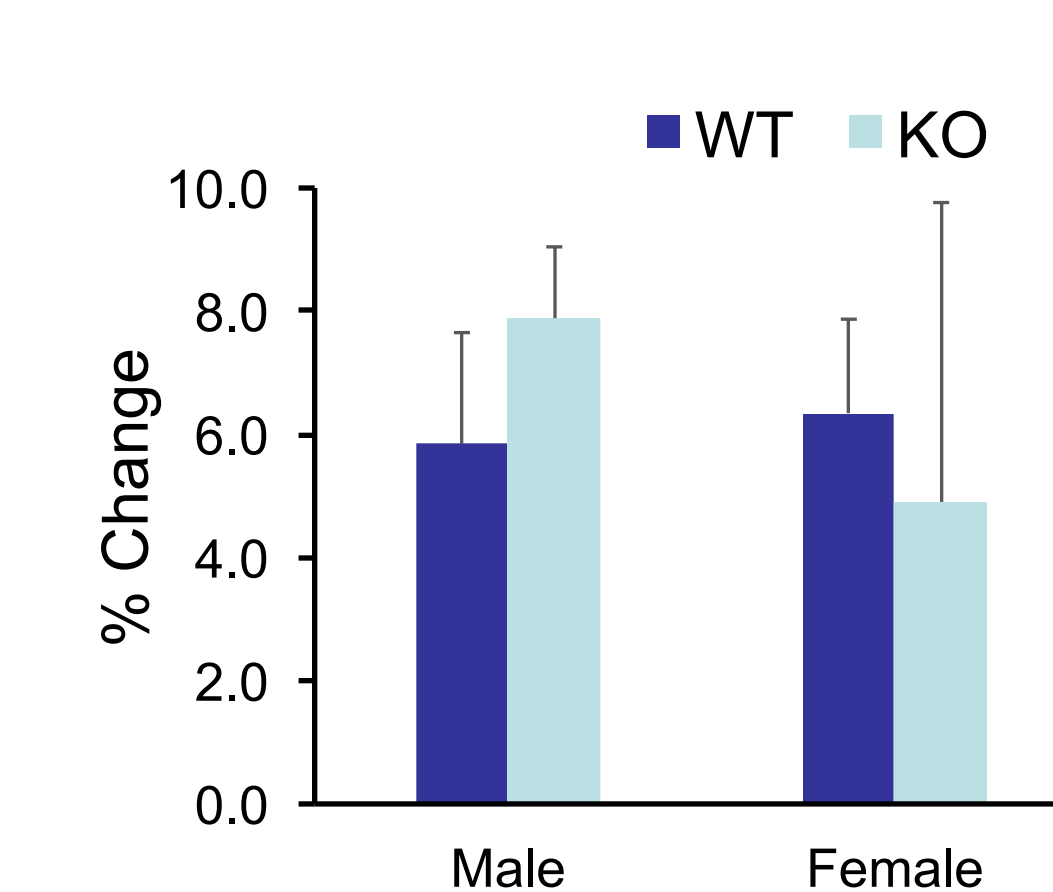


Figure 2. Percent change in body mass calculated at onset (Pre) and day 4 of (T4) of tamoxifen treatment of CAG-Cre^{ERT2}/Atg12^{flox/flox} mice. WT: vehicle-treated; KO: tamoxifen-treated. Values depicted are means; N=3-4/group. Error bars indicate SD. % change = $100 \times (\text{Mass}_{T4} - \text{Mass}_{Pre}) / \text{Mass}_{Pre}$. Two-way ANOVA indicates no gender and treatment effects on % change in body mass. Treatment: not significant; Gender: not significant; Treatment x Gender: not significant.

Efficiency of Atg12 deletion and confirmation of autophagy impairment in bone

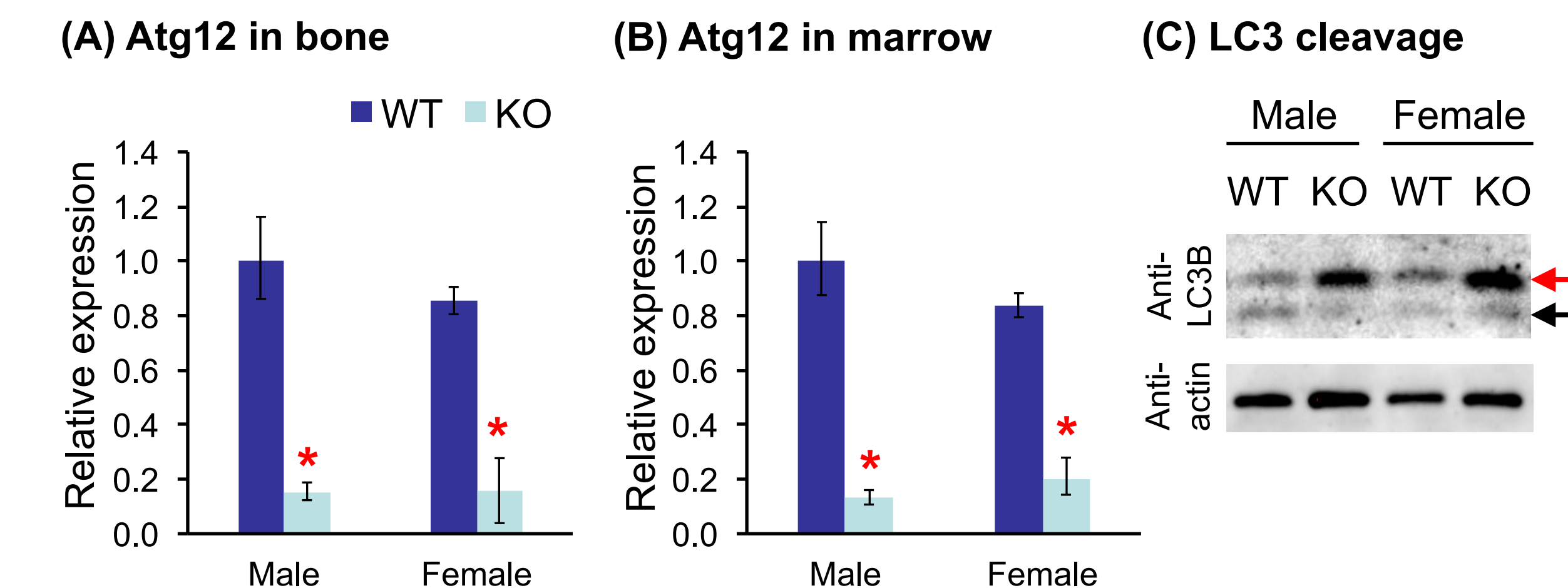


Figure 3. Loss of autophagy after two weeks of tamoxifen treatment of CAG-Cre^{ERT2} / Atg12^{flox/flox} mice. Atg12 expression levels in (A) bone and (B) marrow two weeks after onset of tamoxifen treatment. WT: Vehicle-treated; KO: Tamoxifen-treated. Error bars show upper and lower ranges of relative gene expression levels. *Significant at $p < 0.05$ compared to gender-matched wild type (vehicle-treated) control by two-way ANOVA and Tukey post-hoc test. (C) Western blot showing profound accumulation of LC3B-I (red arrow) and impairments in its cleavage to LC3B-II (black arrow) in bone of KO mice, confirming loss of autophagy. Equal amounts of protein were loaded per well although actin levels appear to change in response to loss of Atg12 (lower blot).

Atg12 deletion favors a pro-osteoclastogenic environment in bone and marrow in a gender-dependent manner

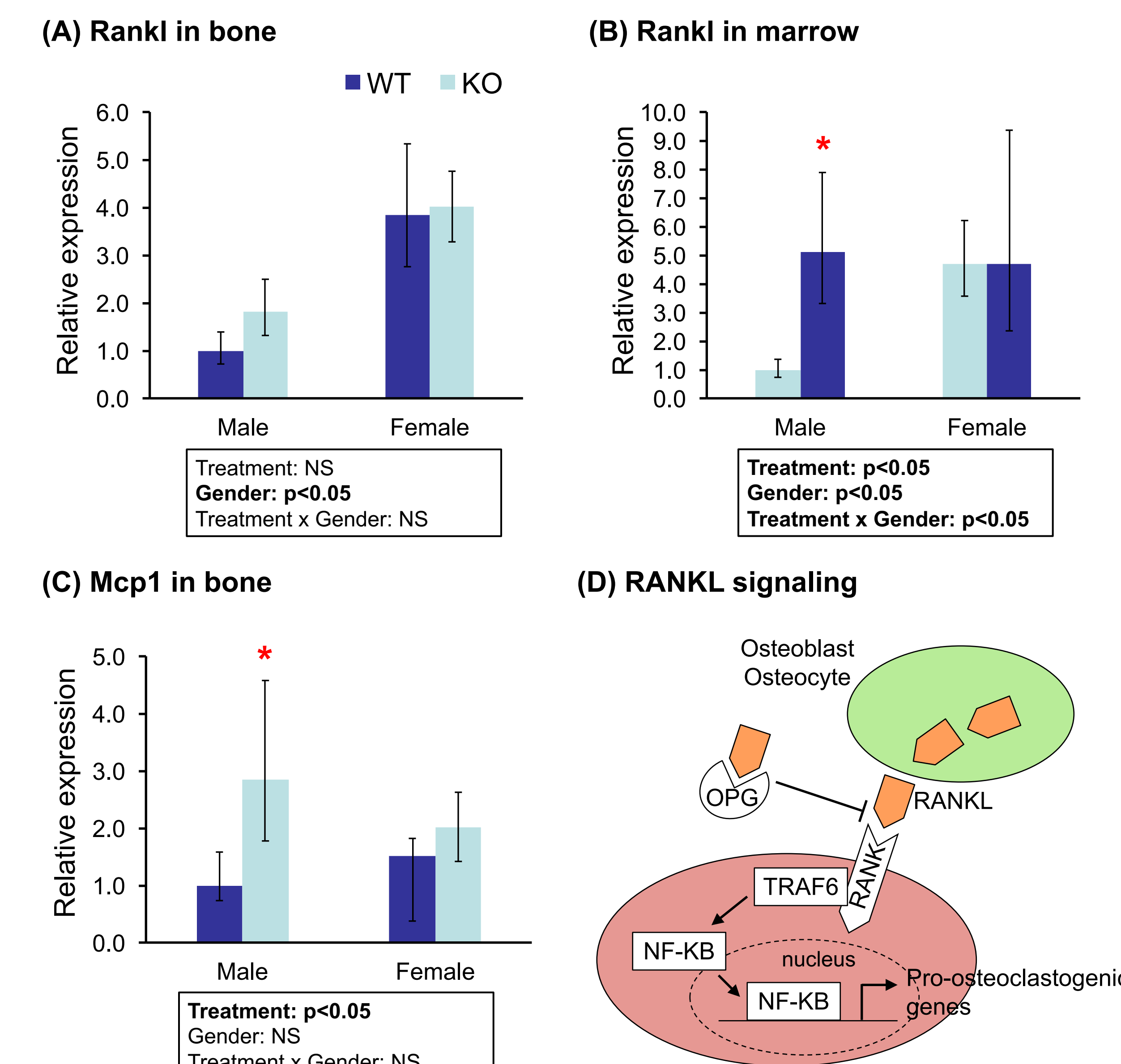


Figure 4. qPCR analyses of Rankl expression in (A) bone and (B) marrow; (C) Mcp1 expression in bone. WT: Vehicle-treated; KO: Tamoxifen-treated. Boxes below graphs indicate results of two-way ANOVA with significance set at $p < 0.05$. NS: Not significant. Error bars show upper and lower ranges of relative gene expression levels. *Significant at $p < 0.05$ compared to gender-matched wild type (vehicle-treated) control by two-way ANOVA and Tukey post-hoc test. (D) *Rankl* encodes a surface-bound molecule on osteoblasts (and osteocytes) that activates osteoclasts. OPG is a decoy receptor that sequesters RANKL and prevents it from binding to its true receptor on osteoclasts, thereby inhibiting osteoclast activity.

Atg12 deletion results in loss of structural integrity of cortical bone; effects more prominent in males

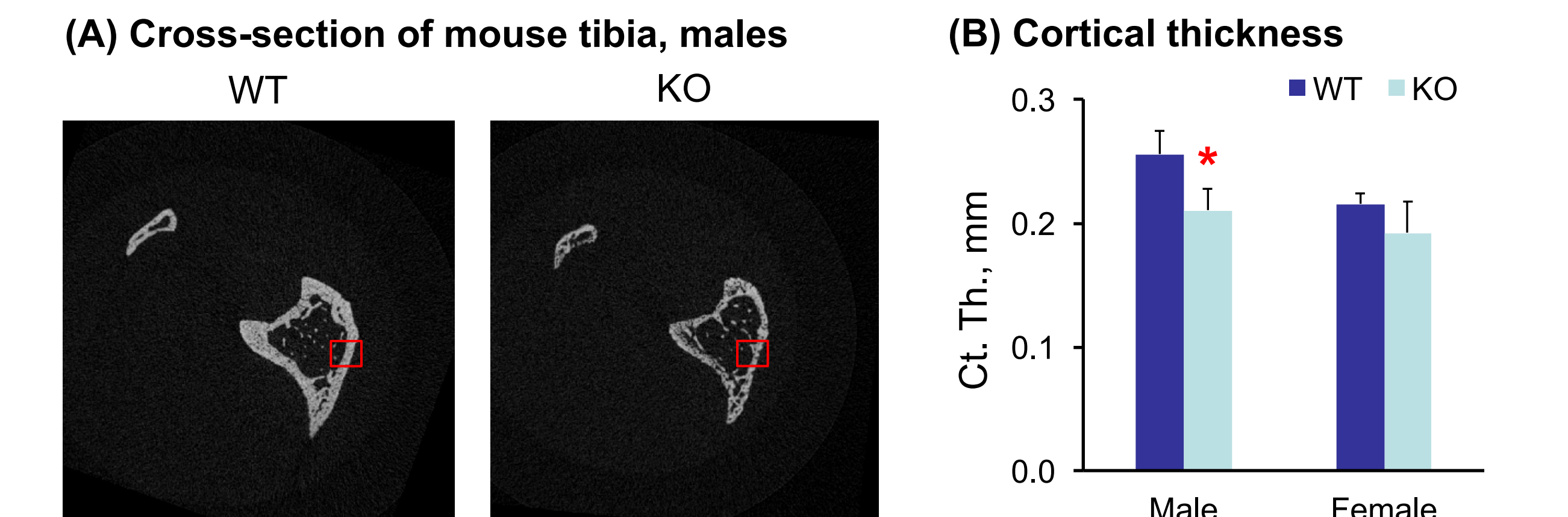


Figure 5. (A) Representative cross sections generated by microCT showing reduced cortical thickness (red rectangle). (B) MicroCT measurements of cortical thickness. Two-way ANOVA indicate Treatment and Gender affects but no Treatment x Gender effects; N=3-4. Error bars show SD. *Significant at $p < 0.05$ compared to gender-matched wild type (vehicle-treated) control by one-way ANOVA.

Cancellous bone is less sensitive to Atg12 deletion

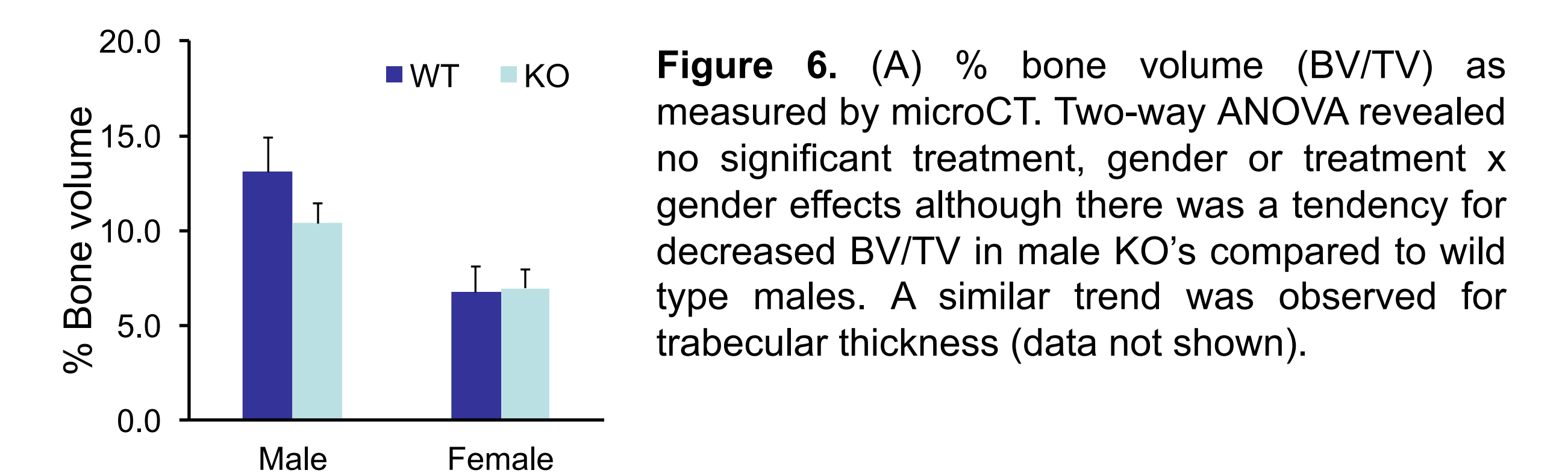


Figure 6. (A) % bone volume (BV/TV) as measured by microCT. Two-way ANOVA revealed no significant treatment, gender or treatment x gender effects although there was a tendency for decreased BV/TV in male KO's compared to wild type males. A similar trend was observed for trabecular thickness (data not shown).

Atg12 deletion leads to altered chondrocyte structure in the growth plate

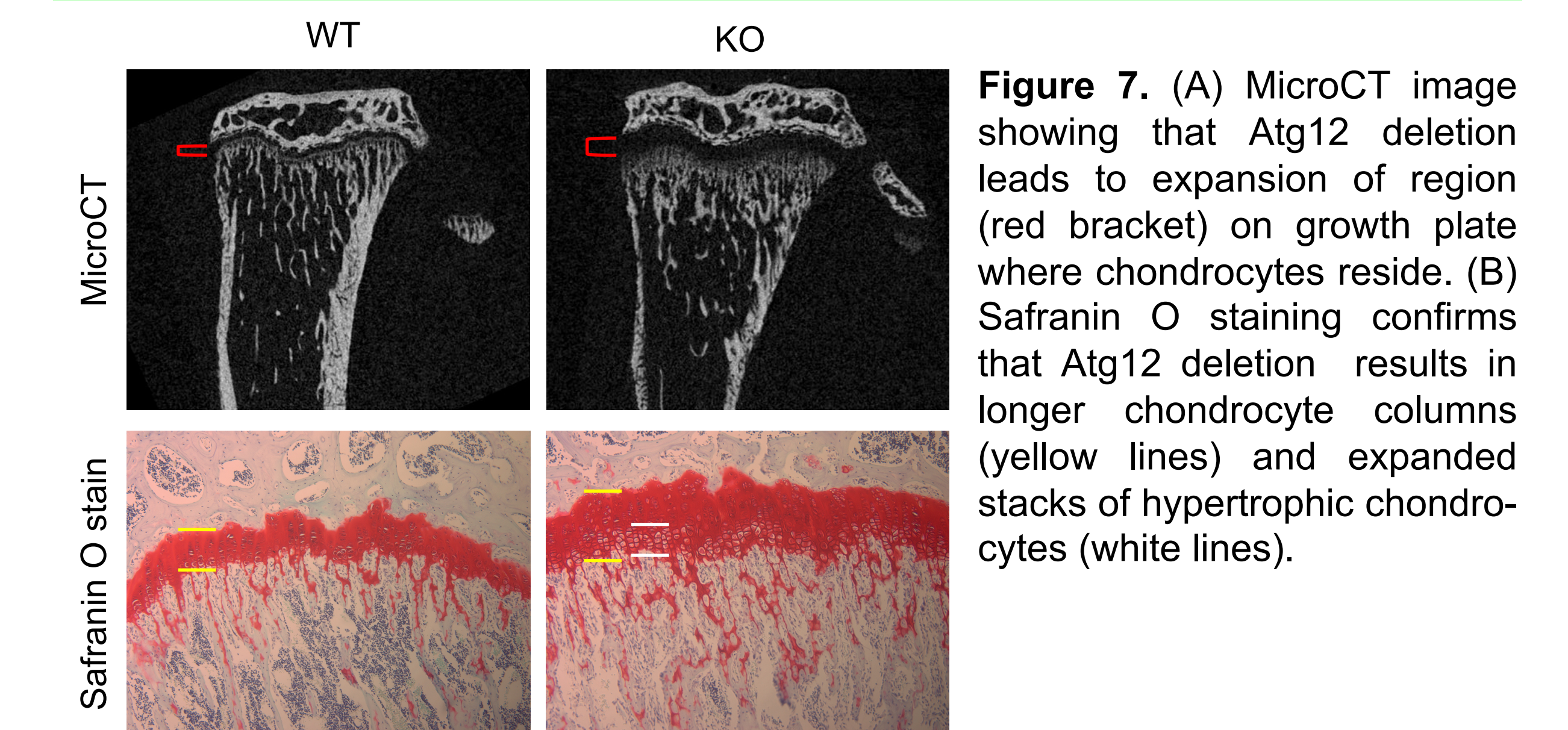


Figure 7. (A) MicroCT image showing that Atg12 deletion leads to expansion of region (red bracket) on growth plate where chondrocytes reside. (B) Safranin O staining confirms that Atg12 deletion results in longer chondrocyte columns (yellow lines) and expanded stacks of hypertrophic chondrocytes (white lines).

CONCLUSION

Loss of autophagy via Atg12 deletion (1) perturbs signals that regulate bone homeostasis, favoring a pro-osteoclastogenic environment, ultimately leading to net bone loss and (2) disrupts chondrocyte proliferation and differentiation. The male skeleton is more sensitive to effects of autophagy deletion.

Acknowledgments: We thank Dr. J. Alwood for advice on microCT analysis. We are grateful to Ali Bahadur for assistance on microCT scanning. This study is supported by the National Space Biomedical Research Institute (NSBRI) through NCC 9-58, Project MA02501 to R.K.G. V.E.R was supported by SLSTP.